Carbohydrate Polymers 148 (2016) 134–142

Contents lists available at ScienceDirect

Carbohydrate Polymers

journal homepage: www.elsevier.com/locate/carbpol

Chitosan-starch beads prepared by ionotropic gelation as potential matrices for controlled release of fertilizers

Jonas J. Perez [a,b,c], Nora J. Francois [a,b,*]

[a] Grupo de Aplicaciones de Materiales Biocompatibles, Departamento de Química, Facultad de Ingeniería, Universidad de Buenos Aires (UBA), Argentina
[b] Instituto de Tecnología en Polímeros y Nanotecnología (ITPN), UBA-CONICET, Argentina
[c] Consejo Nacional de Investigaciones Científicas y Técnicas (CONICET), Argentina

ARTICLE INFO

Article history:
Received 3 December 2015
Received in revised form 9 April 2016
Accepted 11 April 2016
Available online 13 April 2016

Keywords:
Chitosan
Starch
Macrospheres
Fertilizer

ABSTRACT

The present study examines the agrochemical application of macrospheres prepared with chitosan and chitosan-starch blends by an easy dripping technique, using a sodium tripolyphosphate aqueous solution as the crosslinking agent. These biopolymers form hydrogels that could be a viable alternative method to obtain controlled-release fertilizers (CRFs). Three different concentrations (ranging from 20 to 100 wt/wt% of chitosan) and two crosslinking times (2 or 4 h) were used. The resulting polymeric matrices were examined by scanning electron microscopy coupled with energy dispersive X-ray, X-ray diffraction, Fourier transform infrared spectroscopy, solid-state nuclear magnetic resonance, thermogravimetric analysis and differential scanning calorimetry. Ionotropic gelation and neutralization induced the formation of the macrospheres. The crosslinking time and the composition of the polymeric hydrogel controlled the crosslinking degree, the swelling behavior and the fertilizer loading capability. Potassium nitrate-loaded beads were shown to be useful as a controlled-release fertilizer. After 14 days of continuous release into distilled water, the cumulative concentration in the release medium reached between 70 and 93% of the initially loaded salt, depending on the matrix used. The prepared beads showed properties that make them suitable for use in the agrochemical industry as CRFs.

© 2016 Elsevier Ltd. All rights reserved.

1. Introduction

Agriculture is strongly dependent on the addition of fertilizers. Extensive usage of fertilizers has been associated with pollution caused by high levels of nutrients in the ground and surface waters (Valiela et al., 1992; Carpenter et al., 1998; Shaviv & Mikkelsen, 1993), causing health and environmental problems and increasing water purification costs (Carpenter et al., 1998).

On the other hand, the degradation of soil quality after many cycles of intensive agricultural use leads to an increased demand for fertilization, irrigation and energy to maintain the productivity of those soils (Valiela et al., 1992; Carpenter et al., 1998; Shaviv & Mikkelsen, 1993).

One approach to reduce the problems associated with the excessive use of fertilizers is to devise a method that will reduce the quantity and frequency of its application (Chien, Prochnow, & Cantarella, 2009). One way to achieve this goal is to use controlled-release fertilizers (CRFs). These agrochemicals use a physical barrier to reduce the dissolution rate of the fertilizers. Their physical characteristics (reservoir or matrix system), along with the mechanism that governs the fertilizer release (diffusion, swelling or degradation of the polymeric matrix), can modulate the release pattern of nutrients (Rashidzadeh, Olad, Salari, & Reyhanitabar, 2014; Zhong et al., 2013; Shaviv, 2001).

Cost is an important parameter when analyzing the viability of CRFs for industrial manufacturing. For instance, the production of CRFs using hydrogels as carrier matrices still has a considerably higher cost than the use of conventional mineral fertilizers (Rashidzadeh et al., 2014; Zhong et al., 2013). Some polymers can be characterized as "low cost," as they require little processing, are abundant in nature and/or are byproducts or waste materials from other industrial processes. Attempts to use hydrophilic biopolymers to prepare CRFs have been well-documented and reviewed; however, their high cost/benefit ratio hinders their wide use in agriculture. (Jamnongkan & Kaewpirom, 2010; Melaj & Daraio, 2013; Azeem, KuShaari, Man, Basit, & Thanh, 2014).

On the other hand, low-cost synthetic polymers currently used for CRFs often have extremely slow or no decomposition in the soil

* Corresponding author.
E-mail address: nfranco@fi.uba.ar (N.J. Francois).

http://dx.doi.org/10.1016/j.carbpol.2016.04.054
0144-8617/© 2016 Elsevier Ltd. All rights reserved.

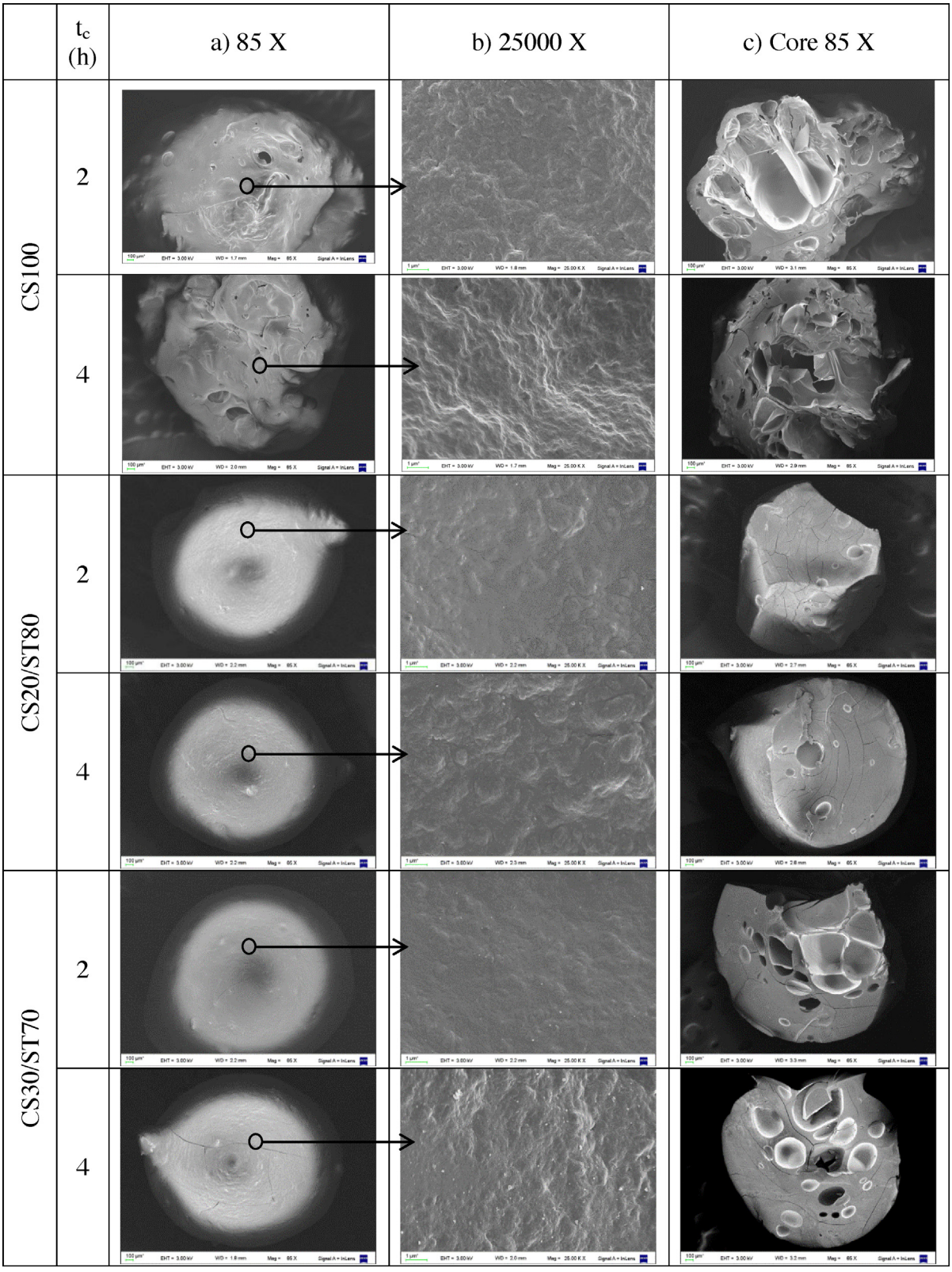

Fig. 1. Scanning electron micrographs of beads prepared with 2 or 4 h of crosslinking time: (a) the entire bead, (b) the external surface and (c) a cross-section are shown.

(Ni, Lü, & Liu, 2012; Davidson & Gu, 2012; Trenkel, 1997), resulting in an accumulation of non-degradable residues. Taking this enormous disadvantage into account, the use of biodegradable polymers would offer an excellent solution to the problem.

Among hydrophilic polymers, we have selected two biodegradable polysaccharides, chitosan and potato starch, that fulfill the desired expectations of low cost, non-polluting characteristics and the ability to modulate fertilizer release.

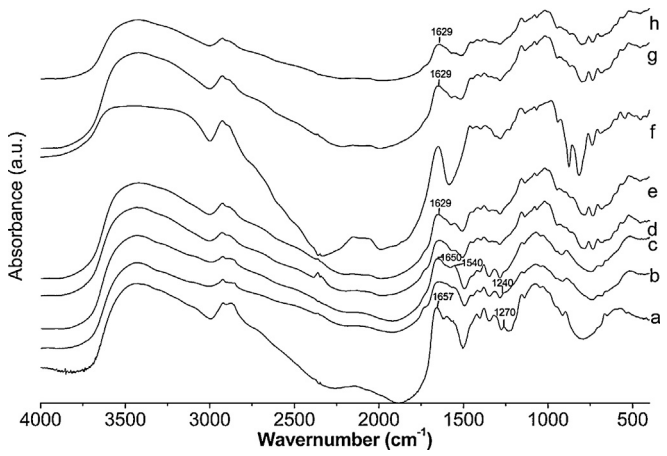

Fig. 2. FTIR spectra of (a) chitosan, (b) CS100 with t_c = 2 h, (c) CS100, t_c = 4 h (d) CS30/ST70 with t_c = 2 h, (e) CS30/ST70 with t_c = 4 h, (f) CS20/ST80 with t_c = 2 h, (g) CS20/ST80 with t_c = 4 h and (h) ST.

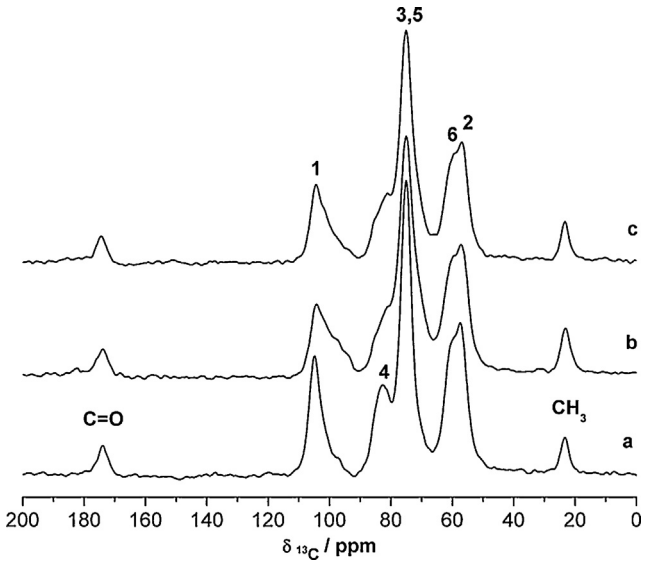

Fig. 3. 13C CP-MAS NMR spectra of chitosan (a), CS100 with t_c = 2 h (b) and CS100 with t_c = 4 h (c).

Chitosan is a linear polysaccharide consisting of β(1 → 4) linked D-glucosamine residues with a variable number of randomly located *N*-acetyl-glucosamine groups (Krajewska, 2004). It is the most important derivative of chitin, which is the main constituent of the crustacean exoskeleton. It is obtained from partial deacetylation of chitin under alkaline conditions or enzymatic hydrolysis in the presence of a chitin deacetylase (Krajewska, 2004; George & Abraham, 2006). Chitosan is a cationic, biocompatible, biodegradable and non-toxic polymer (Kean & Thanou, 2010a, 2010b) that forms ionic complexes with a wide variety of water-soluble anionic polymers or with anionic crosslinking agents, allowing the formation of an insoluble gel (George & Abraham, 2006). It can be chemically crosslinked with reagents, such as glutaraldehyde, genipin or epichlorohydrin (Jose et al., 2012). In this study, physical crosslinking by electrostatic interactions with sodium tripolyphosphate was selected instead of chemical crosslinking in order to avoid the possibility of soil contamination with unreacted chemical crosslinkers. In addition to all of the properties already mentioned, chitosan has excellent properties for agriculture applications because it is a plant growth promoter and also protects against the actions of certain microorganisms (Jose et al., 2012; Nge et al., 2006; Bautista-Baños et al., 2006). On the other hand, its cost significantly diminishes its potential for application in the agrochemical industry.

To produce a low-cost matrix useful for the development of a controlled-release fertilizer based on an ionically crosslinked chitosan, a blend of chitosan and starch was studied. Starch possesses desirable properties, such as compatibility, hydrophilicity, biodegradability, non-toxicity and low-cost (Frost, Kaminski, Kirwan, Lascaris, & Shanks, 2009). Using these blends, much lower quantities of chitosan are needed to prepare the agrochemical.

Starch is a complex natural non-ionic polysaccharide consisting of two polymer fractions that vary widely according to the starch source. The first fraction is a linear polymer called amylose, which is made of β(1 → 4) linked D-glucose, and the second is a branched polymer named amylopectin, which contains the same monomers that are also joined by C1–C6 linkages (Tripathi & Dubey, 2004; Pavlovic & Brandao, 2003; Rindlav-Westling, Stading, & Gatenholm, 2002).

Therefore, the aim of this study was to investigate the feasibility of a simple method of preparing non-polluting hydrogels based on blends of chitosan and starch to be used in the agricultural industry as matrices for the controlled-release of fertilizers. Macrospheres were prepared by ionotropic crosslinking of chitosan using sodium tripolyphosphate. The preparation conditions (crosslinking time and composition of the blends) were analyzed to produce low-cost macrospheres with the lowest possible content of chitosan. The prepared hydrogels were characterized to elucidate their structural, thermal and morphological properties. The final structure of the beads determined their behavior during swelling, which is the main determinant of their fertilizer loading capability and release kinetics.

2. Materials and methods

2.1. Materials

Chitosan of medium molecular weight (81% degree of deacetylation), native potato starch and sodium tripolyphosphate (85% purity) were purchased from Sigma-Aldrich (USA). Lactic acid (85% wt/wt) and potassium nitrate were purchased from Cicarelli (Argentina). All reagents used were of analytical grade and used as received.

2.2. Preparation of macrospheres

A 3% wt/wt chitosan solution was prepared by dissolving chitosan (CS) powder in an aqueous solution of lactic acid (1% v/v) with mechanical stirring.

The potato starch gel was prepared by heating an 8% wt/v starch (ST) solution in deionized water with constant magnetic stirring. Gelatinization was achieved at 76 °C in a boiling distilled water bath.

The crosslinking solution was prepared by dissolving sodium tripolyphosphate (TPP) in distilled water to produce a final concentration of 1% wt/v (pH 8.6).

The blends were prepared by mixing the solution of chitosan and the starch gel with mechanical stirring. Blends were prepared with CS/ST mass ratios of 100/0 (CS100), 30/70 (30CS/70ST) and 20/80 (20CS/80ST).

After they were obtained, the blends were kept at room temperature for 30 min before preparing the beads using a dripping technique. The CS solution and the CS/ST blends were dripped into the TPP solution using plastic tips. After 2 or 4 h of continuous stirring at room temperature, the macrospheres were removed from the TPP solution and extensively washed with distilled water. To ensure complete cleaning, after a drying process at low

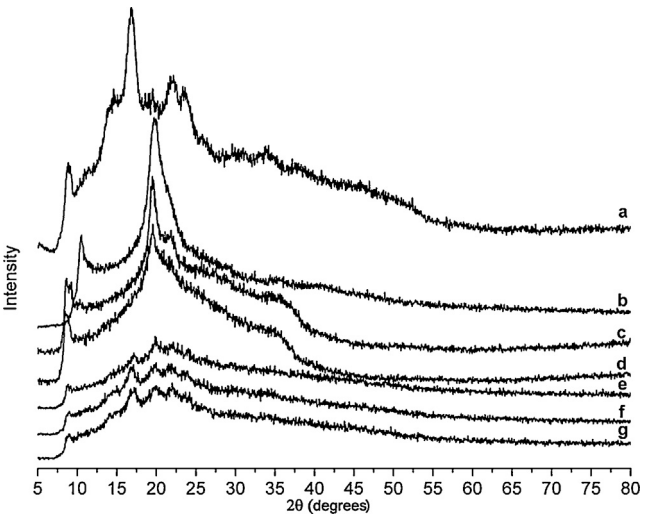

Fig. 4. X-ray diffractograms of starch (a), chitosan (b), CS100 with t_c = 4 h (c), CS100 with t_c = 2 h (d), CS30/ST70 with t_c = 4 h (e), CS20/ST80 with t_c = 4 h (f) and CS20/ST80 with t_c = 2 h (g).

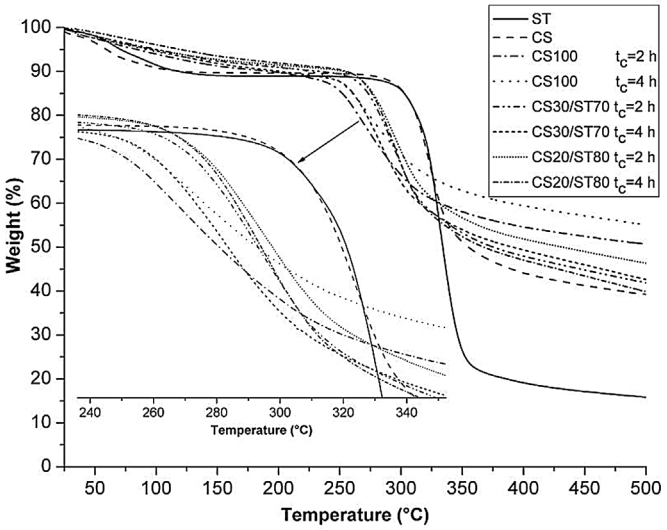

Fig. 5. TGA curves of chitosan, starch, and CS100 with t_c = 2 h, CS100 with t_c = 4 h, CS30/ST70 with t_c = 2 h, CS30/ST70 with t_c = 4 h, CS20/ST80 with t_c = 2 h and CS20/ST80 with t_c = 4 h.

temperature, the macrospheres were rehydrated for 3 h under magnetic stirring and finally dried at 40 °C for 48 h.

2.3. Soluble fraction

A known mass of dried beads was put into a 200 mesh stainless steel spherical net. After being immersed in distilled water for 3 h with magnetic stirring, the samples were dried at 40 °C for 48 h and weighed. The soluble fraction was defined as the ratio between the mass lost as a consequence of the water immersion and the initial mass of the dried material before immersion.

$$\text{Solublefraction\%} = \left(1\text{-}\left(\frac{\text{finaldriedhydrogelmassweight}}{\text{initialwasweightothemacrosphere}}\right)\right) \times 100 \quad (1)$$

2.4. Characterization

2.4.1. Scanning electron microscopy (SEM) with energy dispersive X-ray analysis (EDS)

Crosslinked chitosan and chitosan-starch macrospheres were mounted on aluminum stubs with double-sided adhesive tape and sputter-coated with gold. The surface morphology was examined with a Karl Zeiss Supra 40 SEM (Germany) with a field emission gun operated at 3 kV. The micrographs were taken at magnifications between 70 and 25,000×. Elemental analysis was performed using an Oxford Instruments EDS (United Kingdom) coupled to SEM.

2.4.2. X-ray diffraction (XRD)

XRD patterns were obtained using a Rigaku diffractometer with Bragg Brentano geometry and CuKα radiation (λ = 0.1542 nm, 40 kV, 20 mA) in the range of 2θ = 5–50 at a scanning rate of 1°/min and a scan step of 0.05°. The chart speed was set to 5°/min. Measurements were performed at ambient conditions.

2.4.3. Fourier transform infrared spectroscopy (FTIR)

FTIR spectra of pure chitosan, pure starch and chitosan and chitosan-starch macrospheres were recorded on a Nicolet 380 FTIR spectrometer (Thermo Scientific, Japan) operating in the range of 4000–400 cm^{-1} at a resolution of 4 cm^{-1}. The samples were ground and mixed thoroughly with potassium bromide at a 1:20 (sample:KBr) mass ratio. KBr discs were prepared by compressing the powder mixture with a hydraulic press.

2.4.4. Nuclear magnetic resonance (NMR)

High-resolution ^{13}C solid-state spectra were recorded using the ramp ^{1}H–^{13}C and the combined techniques of proton dipolar decoupling (DD), magic angle spinning (MAS) and cross polarization (CP). Experiments were performed at room temperature in a Bruker Avance II-300 spectrometer equipped with a 4-mm MAS probe. The operating frequency for carbons was 300.13 MHz. Glycine was used as an external reference for the ^{13}C spectra, and the Hartmann–Hahn matching condition was set in the cross-polarization experiments ^{13}C spectra. The recycling time was 4 s. Different contact times during CP were employed in the range of 200–1500 μs for ^{13}C spectra.

2.4.5. Differential scanning calorimetry (DSC)

Thermograms of chitosan, starch, cross-linked chitosan and chitosan-starch macrospheres were obtained with a Shimadzu DSC-60-Plus instrument (Japan). The samples were hermetically sealed in aluminum pans and heated at a constant rate of 10 °C/min. The DSC tracings were performed from 25 to 350 °C. An inert atmosphere was maintained by injecting nitrogen at a flow rate of 30 mL/min.

2.4.6. Thermogravimetric analysis (TGA)

Thermal degradation processes were investigated using a Shimadzu TGA-50 (Japan). Measurements were carried out by heating the sample from 25 to 500 °C under an inert atmosphere maintained by injecting N_2 at a flow rate of 30 mL/min, with a heating rate of 10 °C/min and using a sample weight of approximately 10 mg.

2.4.7. Equilibrium swelling

A known weight of macrospheres was dried to a constant value and then immersed in distilled water at room temperature. The experimental equilibrium swelling degree (Q_ε) was calculated as:

$$Q_\varepsilon = \frac{wt_\varepsilon}{wt_o} x100 \quad (2)$$

where, wt_ε is the weight of the swelled macrospheres at equilibrium and wt_o is the weight of the dry polymeric matrix before the swelling process.

Table 1
Soluble fraction and EDS analysis of CS100, CS30/ST70 and CS20/ST80 prepared hydrogels by different t_c.

t_c (h)	Sample	Soluble Fraction%	Phosphorous wt%
2	**CS100**	7.2 ± 0.2	3.4 ± 0.3
4		6.5 ± 0.3	5.3 ± 0.4
2	**CS30/ST70**	10.9 ± 0.4	2.0 ± 0.2
4		7.5 ± 0.5	2.7 ± 0.3
2	**CS20/ST80**	11.2 ± 0.5	1.4 ± 0.2
4		9.5 ± 0.4	2.4 ± 0.3

Table 2
Equilibrium swelling ratio, maximum loading capacity and temperatures of the maximum degradation rate for macrospheres.

t_c (h)	Samples	Q_e	%KNO_3 loaded (wt/wt)	T_{max} (°C)
2	**CS100**	162.9 ± 2.9	53.3 ± 1.6	278.4 ± 1.8
4		142.6 ± 1.9	49.8 ± 0.9	273.4 ± 1.2
2	**CS30/ST70**	136.0 ± 1.4	40.4 ± 0.8	281.9 ± 1.2
4		120.9 ± 1.9	37.9 ± 1.3	278.7 ± 1.8
2	**CS20/ST80**	151.0 ± 1.6	41.1 ± 1.9	293.3 ± 1.9
4		133.6 ± 1.5	36.7 ± 1.2	292.2 ± 1.5

2.4.8. Loading of potassium nitrate

Potassium nitrate in powder form was dissolved in deionized water at a final concentration of 20% wt/wt. Dry polymeric matrices were immersed in the fertilizer-saturated aqueous solution for 4 h at room temperature. After the swelling process, the macrospheres were dried at 40 °C for 48 h. The loading percentage was calculated using the following equation:

$$\%Loaded = \frac{wt_f - wt_o}{wt_o} x100 \quad (3)$$

where wt_f and wt_o are the weights of the loaded and unloaded dry macrospheres, respectively.

2.4.9. Release tests

The release of potassium nitrate-loaded in the matrices was performed using deionized water as the release medium. A constant fixed weight of loaded beads was placed inside a steel basket that was immersed in 100 mL of deionized water at a constant temperature of 25 °C under un-stirred conditions (static experiment). At fixed time intervals, the cumulative concentration of KNO_3 released was evaluated by measuring the conductivity of the release medium with a Hanna Instruments HI 9033 multi-range conductivity meter. The cumulative concentration of KNO_3 was determined from the calibration plot.

2.5. Statistical analyses

The values reported are the means and standard deviations of experiments carried out at least three times. Data were analyzed using a one-way analysis of variance (*t*-test), and $p < 0.05$ was considered significant.

3. Results and discussion

3.1. Soluble fraction

As a consequence of the TPP dissolution and hydrolysis, the aqueous crosslinking solution possesses OH^- and tripolyphosphoric ions. Both ions can diffuse into hydrogels when the polymeric material is in contact with the aqueous TPP solution. The OH^- ions compete with $P_3O_{10}^{5-}$ ions for reaction with the protonated amino group of chitosan as soon as the polymeric droplets come into contact with the sodium tripolyphosphate solution.

Taking into account that ionic crosslinking can be controlled by adjusting the pH of the TPP aqueous solution, a pH of 8.6 was chosen in order to achieve a low crosslinking density in the polymeric matrix (Mi, Shyu, Lee, & Wong, 1999; Shu & Zhu, 2001).

The macrospheres prepared from chitosan and from blends maintained their integrity (did not dissolve or break apart) during the experiment. The calculated soluble fraction is directly related to the selected polymeric composition and crosslinking time. The soluble fractions are shown in Table 1.

A slight decrease in the soluble fraction was observed when the crosslinking time or the chitosan content were increased. Bourtoom & Chinnan (2008) obtained similar experimental results by preparing films made of rice starch-chitosan blends. They reported a decrease in the soluble fraction with the augmentation of the CS wt% that could be attributable to the interactions between both biopolymers. When the CS percent or the crosslinking time (t_c) are lowered, the ionic crosslinking between CS chains decreases, and the interactions between biopolymers are affected, producing a larger soluble fraction.

3.2. SEM and EDS analysis

EDS was used to analyze the phosphorus content on the external surface of the macrospheres after 2 or 4 h of cross-linking in order to obtain information about the effectiveness of the crosslinking. An increase in the amount of phosphorus would confirm an increase in the crosslinking density (Mi et al., 1999). The phosphorus wt% measured on the external surface of different matrices is shown in Table 1. The semi-quantitative results revealed that the content of phosphorus is highly dependent on the t_c. The experimental results are in agreement with the lower crosslinking degree achieved at the minimum t_c tested.

It is also observed that this phosphorus wt% decreased after incorporation of ST. This fact could indicate that, in the case of matrices prepared from blends, the added ST is not involved in the ionic crosslinking with TPP. Using a room temperature setting in the preparation method of macrospheres eliminates the possibility of a crosslinking reaction between ST and TPP, which only would occur at a high temperature (>100 °C) (Deetae et al., 2008; Lim & Seib, 1993).

Fig. 1 shows the morphology of dried samples prepared with chitosan or polymeric blends with different crosslinking times. The bead diameters, regardless the crosslinking time, are 3.70 ± 0.03 mm for chitosan beads and 3.00 ± 0.05 mm for matrices

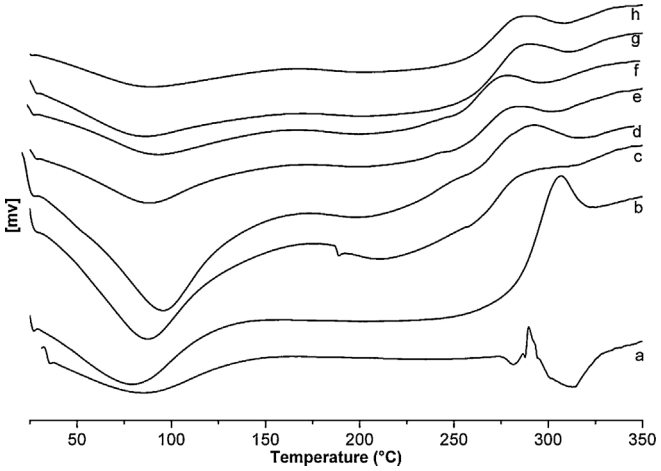

Fig. 6. DSC thermograms of chitosan (a), starch (b), CS100 with t_c = 2 h (c), CS100 with t_c = 4 h (d), CS30/ST70 with t_c = 2 h (e), CS30/ST70 with t_c = 4 h (f), CS20/ST80 with t_c = 2 h (g) and CS20/ST80 with t_c = 4 h (h).

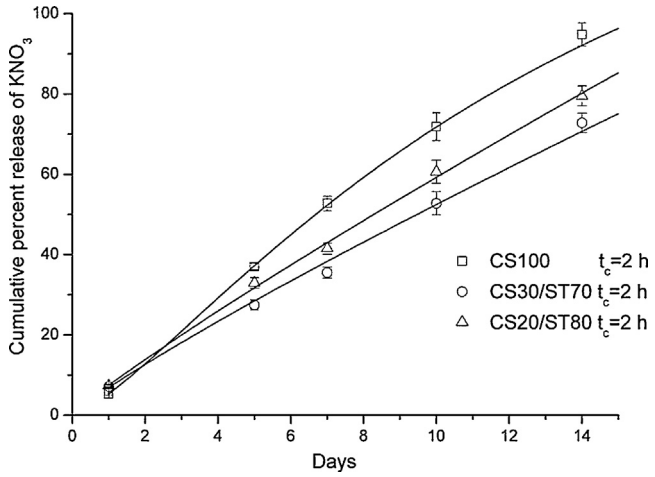

Fig. 7. Cumulative percent release of KNO_3 as a function of time from matrices prepared with a t_c = 2 h.

prepared with blends. These sizes are optimal for a final agrochemical application.

Other general properties were observed, including the findings that none of the analyzed macrospheres were completely spherical in shape and that the crosslinking time does not significantly affect the final size. According to the experimental procedure, the main factor that would affect the size of the beads is the diameter of the plastic tip used in the dripping technique.

The micrographs of the surfaces of the cross-sectioned beads show many cavities of different sizes. The presence of these cavities could be caused by the preparation method. They could be the consequence of occluded air bubbles incorporated during the preparation of the polymeric material used to manufacture the beads. The observed inner structure is useful in the preparation of a controlled-release fertilizer because it would enhance the loading of the fertilizer inside the polymeric matrix.

In accordance with previous reports (Mi et al., 1999; Shu & Zhu, 2001), the pH chosen for the TPP solution used in this work is adequate because, due to the low crosslinking density achieved, it produces porous structures.

3.3. FTIR results

Fourier transform infrared spectroscopy studies were conducted in order to gain insight into the structural changes of the macrospheres obtained with different compositions and using either 2 or 4 h of crosslinking time. Fig. 2 shows all of the spectra obtained by this method.

The FTIR spectrum of potato starch showed common features of polysaccharides. An intense band at 1653 cm^{-1} was assigned to the O—H bending vibration (Capron, Robert, Colonna, Brogly, & Planchot, 2007; Fang, Fowler, Tomkinson, & Hill, 2002; Iizuka & Aishima, 1999). The bands at 1151 and 2930 cm^{-1} correspond to the C—O and C—H stretching regions (Capron et al., 2007; Fang et al., 2002). The 3380–3420 cm^{-1} region (Capron et al., 2007) shows the weakest stretching frequency, that of the O—H band (Capron et al., 2007; Fang et al., 2002).

The pure chitosan spectrum presented a characteristic band at 3449 cm^{-1} that is attributed to an overlap of the stretching vibrations of the —NH_2 and —OH groups. There is a band located at 1657 cm^{-1} for amide I (Cui et al., 2008; Zawadzki & Kaczmarek, 2010; Pierog, Gierszewska-Drużyńska, & Ostrowska-Czubenko, 2009; Pawlak & Mucha, 2003). There is also a band at 1657 cm^{-1} corresponding to the $CONH_2$ group and a signal at 1598 cm^{-1} due to the NH_2 group (Bhumkar & Pokharkar, 2006; Mi et al., 1999; Pierog et al., 2009).

Macrospheres prepared with only chitosan showed a shoulder at 1240 cm^{-1}, which can be assigned to the —P═O stretching vibration, indicating the presence of the phosphate group as a consequence of ionic crosslinking (Bhumkar & Pokharkar, 2006; Mi et al., 1999; Pierog et al., 2009). It was found that the intensity of this shoulder increased with increasing crosslinking time.

A comparison of the chitosan spectrum with that of the chitosan macrospheres shows that the peak at 1657 cm^{-1} disappeared after gelation, and two new peaks, at 1650 cm^{-1} and 1540 cm^{-1}, appeared in the spectrum after 2 or 4 h of crosslinking. This can be attributed to the linkage between the polyphosphoric and protonated amino ions (Bhumkar & Pokharkar, 2006; Qi, Xu, Jiang, Hu, & Zou, 2004; Qi & Xu, 2004). Additionally, the intensity of the peak at 1540 cm^{-1} increased with increasing crosslinking time, suggesting a higher crosslinking density (Mi et al., 1999).

The starch gelatinization causes exposure of the OH groups. It has been established that these groups can form hydrogen bonds with the protonated amino groups of chitosan (Mathew, Brahmakumar, & Abraham, 2006; Pelissari, Grossmann, Yamashita, & Pineda, 2009; Wang, Zhang, Hu, Yang, & Du, 2007). These interactions causes changes in the spectra corresponding to the chitosan/starch hydrogels, as the amino group peak of chitosan shifted from 1657 to 1629 cm^{-1}. These changes are evidence of the good molecular compatibility between the biopolymers selected to produce the macrospheres.

The FTIR spectra of matrices obtained from blends also revealed a shoulder at 1240 cm^{-1}, demonstrating the existence of the —P═O group and indicating that crosslinking took place through ionic interactions between the negatively charged —P═O group and the NH_3^+ group in chitosan.

3.4. NMR assays

NMR was conducted using on the chitosan beads in order to analyze the influence of the crosslinking time on the ionic crosslinking produced between chitosan and TPP.

The CP-MAS ^{13}C NMR spectrum for chitosan, shown in Fig. 3, was very similar to that reported in the literature (Barbi et al., 2015). The following characteristic signals can be identified: d = 60 ppm (two convoluted signals are observed and attributed to carbon C6 and C2); d = 76.4 ppm (carbons C5 and C3); d = 84 ppm (carbon C4) and d = 106.2 ppm (carbon C1). It was found that for peaks corresponding to the C1 and C4 positions decreased in intensity and became broader than the original signals, indicating that the interaction between CS and TPP effectively occurred during the creation of the polymeric matrices. A stronger interaction is observed when the crosslinking time is increased.

3.5. XRD studies

XRD diffractograms of pure chitosan, pure starch and macrospheres prepared with chitosan or blends are shown in Fig. 4.

Starch is a semicrystalline polymer. Depending on the starch source, its crystallinity can vary from 15 to 51% (Foresti, Williams, Martínez-García, & Vázquez, 2014).

Potato starch showed typical crystalline peaks centered at 5.75, 16.85, 23.71, 24.16, 30.61 and 35.14°. It exhibited the characteristic 'B' type X-ray pattern of tuber starches (Cheetham & Tao, 1998). Chitosan exhibited two crystalline and defined peaks at 10.55 and 19.7° (Qi et al., 2004). The peaks found in the CS100 diffractogram decreased slightly when the ionic crosslinking time was increased. The crosslinking inhibits a close packing of the polymer chains by reducing the degrees of freedom in the 3-D conformation, limiting

or even preventing the formation of crystalline regions (Qi & Xu, 2004).

The method used to obtain chitosan beads causes simultaneous deprotonation ionic crosslinking of the chitosan chains. This process could produce deprotonated chains but not crosslinked or mobile deprotonated chain segments between crosslinking points, which are capable of a certain rearrangement that could explain the XRD diffractogram of chitosan beads (Bhumkar & Pokharkar, 2006).

In the case of polymeric macrospheres prepared with blends, the XRD pattern showed a decreased intensity of the characteristic peaks corresponding to chitosan and starch, which is indicative of a degree of interaction between the molecular chains of both polysaccharides (Xu, Kim, Hanna, & Nag, 2005).

As the starch/chitosan ratio increases, there are more OH groups from the starch polymeric chains that are able to interact with chitosan's protonated amino groups. This increased interaction between biopolymers caused a shift of the chitosan diffraction peak from 10.55° to a lower value and then its disappearance with increasing starch content (Fig. 4(e)–(g)) (Xu et al., 2005).

3.6. Thermal analysis

The thermogravimetric analysis (TGA) results from different samples are shown in Fig. 5.

From the TGA results, is possible to appreciate three different stages. A first stage of weight loss below and approximately 100 °C can be attributed to water evaporation. Polysaccharides usually have a strong affinity for water and, therefore, may be easily hydrated, resulting in macromolecules with rather disordered structures. The hydration properties of these polysaccharides depend on their primary and supra-molecular structure (Kittur, Prashanth, Sankar, & Tharanathan, 2002). In our case, the matrices prepared exclusively with chitosan presented the highest weight loss. The addition of starch caused a decrease in the ionic crosslinking degree because of the lower chitosan concentration and also caused a decrease in the amount of water lost compared to the results obtained from chitosan macrospheres. As a result of the high hydrophilicity of starch, the water retention showed anomalous behavior because it was found that the weight lost at 100 °C was lower in macrospheres prepared from blends. Water can act as a plasticizer for both biopolymers, but in the case of starch, it can increase retrogradation with a consequent increase in crystallinity (Zhiqiang, Xiao-Su, & Yi, 1999). This phenomenon can generate a barrier effect that could prevent the loss of water from the macrospheres obtained from blends.

There is a second stage of weight loss, observed between 240 and 340 °C, that is due to the depolymerization of chitosan and to the decomposition of starch for matrices prepared with blends. This phenomenon can be ascribed to a complex process that includes the dehydration of the saccharide rings and the depolymerization and decomposition of the glucose units belonging to starch (Fang et al., 2002).

Finally, there is a third stage between 340 and 500 °C caused by the pyrolysis of chitosan and the vaporization and elimination of the volatile products of starch (Zawadzki & Kaczmarek, 2010).

The results obtained from the derivative thermogravimetric analysis (dTGA) are shown in Table 2.

The dTGA curves showed that there are differences in the temperature associated with the maximum mass loss rate (T_{max}) for beads of different composition or prepared with different crosslinking times. For macrospheres prepared with blends, the factor that mostly affects the T_{max} is the mass composition. The experimental T_{max} is lower than the value obtained by applying the mixture rule (He, Zhu, & Inoue, 2004). This observation points to the existence of molecular interactions between the biopolymers used, which have already been reported (Mi et al., 1999). Independent of the sample being analyzed, T_{max} always decreased with increasing crosslinking time. This fact could be related to the decrease in crystallinity caused by the increase in ionic crosslinking (Mi et al., 1999). For blend matrices, T_{max} increased with the percentage of starch added, showing higher thermal stability than the samples prepared exclusively with chitosan. This result could be attributed to an increase in crystallinity, as already discussed for the XRD and TGA results.

The DSC curves are shown in Fig. 6. All samples showed an endothermic transition associated with water evaporation in the 50–150 °C range. Regarding the temperature peak of the mentioned transition, increasing t_c caused a shift to higher temperatures because more energy was required to remove water from hydrogels with a greater degree of crosslinking (Sarmento, Ferreira, Veiga, & Ribeiro, 2006).

The chitosan content was a determining factor in the registered temperature shift of the endothermic peak. As the chitosan content increased, the shift was more pronounced because of the increase in the ionic interactions that affected the crystallinity of the matrices, as already discussed with the TGA results. A peak corresponding to exothermic decomposition (depolymerization) is observed for chitosan at 292.78 °C (Choi, Kim, Pak, Yoo, & Chung, 2007), while for the crosslinked matrices, the same transition was observed at lower temperatures but with lower intensity. Ionic crosslinking with TPP led to a decrease in crystallinity, which led to lower thermal stability for chitosan macrospheres than for pure chitosan (Mi et al., 1999; Lee, Mi, Shen, & Shyu, 2001). In the case of macrospheres prepared from blends, it was observed that the temperature shift corresponding to the peak of the exothermic transition was more pronounced than the one registered for crosslinked matrices prepared exclusively with chitosan.

This result could be related to all the interactions occurring in the polymeric blend. By increasing the starch content, the level of ionic crosslinking or the physical interactions via hydrogen bonds between both biopolymers tends to decrease.

TGA and DSC results were indicative of the existence of ionic crosslinking and good compatibility between chitosan and starch macromolecules.

3.7. Swelling and KNO_3 loading assays

Water absorption produces swelling of the tridimensional polymeric network. In the case of beads loaded with potassium nitrate, this phenomenon has a key role in governing fertilizer release (Huanbutta et al., 2011).

Due to the direct relationship between the swelling and the structure of the material, modification of the crosslinking time and/or the polymeric composition of the beads could be an interesting approach for regulating the release of the loaded fertilizer.

The swelling experiments indicated that none of the samples dissolved during the time interval assayed and that all reached an equilibrium swelling capacity after 3 h.

An increase in the crosslinking time induced a decrease of approximately 12% in the swelling degree of all matrices tested, regardless of its polymeric composition (Yalinca, Yilmaz, & Bullici, 2012). This result could be explained by the increase in the ionic interchain linkages (Mi et al., 1999).

In the case of macrospheres prepared using blends at equal t_c, the swelling equilibrium degree is lower than that of the chitosan beads, reaching a minimum when a 30% wt/wt of chitosan is used. The introduction of a certain amount of starch induces changes in the final matrix structure associated with the ionic crosslinking density and with the intermolecular interactions between both biopolymers. XRD, FTIR and TGA results indicate that increasing the starch content affects the interactions within the tridimensional

polymeric network, producing a larger swelling degree accordingly to the results presented in Table 2.

Because of the loading method, a direct relationship between the swelling degree and the loading capacity is expected (Samanta & Ray, 2014). The experimental maximum fertilizer loading shown in Table 2 indicates that chitosan beads possessed a maximum loading capacity in accordance with the higher equilibrium swelling degrees measured for these matrices. Surprisingly, in the case of the beads prepared with both blends, the fertilizer loading capacity was approximately the same. Further studies are being conducted in order to understand this experimental result.

3.8. Release kinetics

To use a conductimetric method to determine the concentration of the loaded fertilizer in the release medium, potassium nitrate was selected because it has pH-independent solubility and does not affect the pH of the release medium. The release kinetics of the loaded beads is directly influenced by the swelling behavior (Samanta & Ray, 2014). For CS100 matrices, the t_c had a significant influence on the release pattern, changing the percentage of cumulative KNO_3 released after 14 days from 95% to 73% when the crosslinking time was changed from two to four hours (experimental results not shown).

Fig. 7 shows the release pattern obtained from matrices prepared with a t_c of two hours. The cumulative percent release was calculated, for each matrix, considering the experimental maximum fertilizer loading (Table 2) as a 100%. After fourteen days, the cumulative concentration of KNO_3 released was 95% for CS100, 73% for CS30/ST70 and 80% for CS20/ST80.

These results correlate with the equilibrium swelling degrees shown in Table 2 because the mechanism of fertilizer release involves swelling of the polymeric matrix when the loaded bead makes contact with water (Rashidzadeh et al., 2014).

There are numerous reports of matrices prepared with hydrogels that are intended to be used as controlled-release fertilizers, but the release was faster than that obtained in this work. For example, Jamnongkan and Kaewpirom prepared a poly(vinyl alcohol)/chitosan hydrogel that released up to 70% of the same fertilizer used in this work over only four days. Liang, Liu, & Wu (2007) prepared a coated fertilizer with a loaded core of alginate that released approximately 90% of the loaded potassium during six days.

Taking into account that the release experiments were conducted immersing the loaded beads in water and observing in Fig. 7 the release profiles of matrices crosslinked over 2 h, it is clear that the developed matrices would be potentially useful as controlled-release fertilizers.

4. Conclusions

Chitosan and chitosan/starch macrospheres can be easily prepared from an ionic crosslinking reaction between chitosan macromolecules using an aqueous TPP solution.

The ionic crosslinking and the starch incorporation produced a decrease in the crystallinity of the material prepared.

FTIR, XRD, TGA and DSC experimental results suggested good molecular compatibility between starch and chitosan.

Swelling experiments, fertilizer loading and release kinetics indicated that the macrospheres prepared with blends are excellent candidates to be used for controlled-release of fertilizer.

This approach to control the properties of hydrogels with various combinations of composition and crosslinking densities may find a wide range of industrial applications, such as in the agroindustry.

Acknowledgments

This work and the data herein contained was supported by Universidad de Buenos Aires, Argentina (Grant 20020130200086BA UBACyT 2014-2017).

References

Azeem, B., KuShaari, K., Man, Z. B., Basit, A., & Thanh, T. H. (2014). Review on materials & methods to produce controlled release coated urea fertilizer. *Journal of Controlled Release*, *181*, 11–21.

Barbi, M. D. S., Carvalho, F. C., Kiill, C. P., Da Silva, B., Santagneli, S. H., Ribeiro, S. J. L., et al. (2015). Preparation and characterization of chitosan nanoparticles for zidovudine nasal delivery. *Journal of Nanoscience and Nanotechnology*, *15*(1), 865–874.

Bautista-Baños, S., Hernández-Lauzardo, A. N., Velázquez-del Valle, M. G., Hernández-López, M., Barka, E. A., Bosquez-Molina, E., et al. (2006). Chitosan as a potential natural compound to control pre and postharvest diseases of horticultural commodities. *Crop Protection*, *25*(2), 108–118.

Bhumkar, D. R., & Pokharkar, V. B. (2006). Studies on effect of pH on cross-linking of chitosan with sodium tripolyphosphate: a technical note. *AAPS Pharmscitech*, *7*(2), E138–E143.

Bourtoom, T., & Chinnan, M. (2008). Preparation and properties of rice starch–chitosan blend biodegradable film. *LWT-Food Science and Technology*, *41*(9), 1633–1641.

Capron, I., Robert, P., Colonna, P., Brogly, M., & Planchot, V. (2007). Starch in rubbery and glassy states by FTIR spectroscopy. *Carbohydrate Polymers*, *68*(2), 249–259.

Carpenter, S., Caraco, N., Correll, D., Howarth, R., Sharpley, A., & Smith, V. (1998). Nonpoint pollution of surface waters with phosphorus and nitrogen. *Ecological Applications*, *8*(3), 559–568.

Cheetham, N. W., & Tao, L. (1998). Variation in crystalline type with amylose content in maize starch granules: an X-ray powder diffraction study. *Carbohydrate Polymers*, *36*(4), 277–284.

Chien, S. H., Prochnow, L. I., & Cantarella, H. (2009). Recent developments of fertilizer production and use to improve nutrient efficiency and minimize environmental impacts. *Advances in Agronomy*, *102*, 267–322.

Choi, C. Y., Kim, S. B., Pak, P. K., Yoo, D. I., & Chung, Y. S. (2007). Effect of N-acylation on structure and properties of chitosan fibers. *Carbohydrate Polymers*, *68*(1), 122–127.

Cui, Z., Xiang, Y., Si, J., Yang, M., Zhang, Q., & Zhang, T. (2008). Ionic interactions between sulfuric acid and chitosan membranes. *Carbohydrate Polymers*, *73*(1), 111–116.

Davidson, D., & Gu, F. (2012). Materials for sustained and controlled release of nutrients and molecules to support plant growth. *Journal of Agricultural and Food Chemistry*, *60*(4), 870–876.

Deetae, P., Shobsngob, S., Varanyanond, W., Chinachoti, P., Naivikul, O., & Varavinit, S. (2008). Preparation, pasting properties and freeze–thaw stability of dual modified crosslink-phosphorylated rice starch. *Carbohydrate Polymers*, *73*(2), 351–358.

Fang, J., Fowler, P., Tomkinson, J., & Hill, C. A. S. (2002). The preparation and characterisation of a series of chemically modified potato starches. *Carbohydrate Polymers*, *47*(3), 245–252.

Foresti, M., Williams, M., Martínez-García, R., & Vázquez, A. (2014). Analysis of a preferential action of α-amylase from B. licheniformis towards amorphous regions of waxy maize starch. *Carbohydrate Polymers.*, *102*, 80–87.

Frost, K., Kaminski, D., Kirwan, G., Lascaris, E., & Shanks, R. (2009). Crystallinity and structure of starch using wide angle X-ray scattering. *Carbohydrate Polymers*, *78*(3), 543–548.

Kean, T., & Thanou, M. (2010). Biodegradation, biodistribution and toxicity of chitosan. *Advanced Drug Delivery Reviews*, *62*(1), 3–11.

George, M., & Abraham, T. E. (2006). Polyionic hydrocolloids for the intestinal delivery of protein drugs: alginate and chitosan—a review. *Journal of Controlled Release*, *114*(1), 1–14.

He, Y., Zhu, B., & Inoue, Y. (2004). Hydrogen bonds in polymer blends. *Progress in Polymer Science*, *29*(10), 1021–1051.

Huanbutta, K., Sriamornsak, P., Limmatvapirat, S., Luangtana-anan, M., Yoshihashi, Y., Yonemochi, E., et al. (2011). Swelling kinetics of spray-dried chitosan acetate assessed by magnetic resonance imaging and their relation to drug release kinetics of chitosan matrix tablets. *European Journal of Pharmaceutics and Biopharmaceutics*, *77*(2), 320–326.

Iizuka, K., & Aishima, T. (1999). Starch Gelation Process Observed by FT-IR/ATR Spectrometry with Multivariate Data Analysis. *Journal of Food Science*, *64*(4), 653–658.

Jamnongkan, T., & Kaewpirom, S. (2010). Potassium release kinetics and water retention of controlled-release fertilizers based on chitosan hydrogels. *Journal of Polymers and the Environment*, *18*(3), 413–421.

Jose, S., Fangueiro, J., Smitha, J., Cinu, T., Chacko, A., Premaletha, K., et al. (2012). Cross-linked chitosan microspheres for oral delivery of insulin: taguchi design and in vivo testing. *Colloids and Surfaces B: Biointerfaces*, *92*, 175–179.

Kean, T., & Thanou, M. (2010). Biodegradation, biodistribution and toxicity of chitosan. *Advanced Drug Delivery Reviews*, *62*(1), 3–11.

Kittur, F. S., Prashanth, K. H., Sankar, K. U., & Tharanathan, R. N. (2002). Characterization of chitin, chitosan and their carboxymethyl derivatives by differential scanning calorimetry. *Carbohydrate Polymers*, *49*(2), 185–193.

Krajewska, B. (2004). Application of chitin-and chitosan-based materials for enzyme immobilizations: a review. *Enzyme and Microbial Technology*, *35*(2), 126–139.
Lee, S. T., Mi, F. L., Shen, Y. J., & Shyu, S. S. (2001). Equilibrium and kinetic studies of copper(II) ion uptake by chitosan-tripolyphosphate chelating resin. *Polymer*, *42*(5), 1879–1892.
Lim, S., & Seib, P. (1993). Preparation and pasting properties of wheat and corn starch phosphates. *Cereal Chemistry*, *70*(2), 137.
Mathew, S., Brahmakumar, M., & Abraham, T. E. (2006). Microstructural imaging and characterization of the mechanical, chemical, thermal, and swelling properties of starch–chitosan blend films. *Biopolymers*, *82*(2), 176–187.
Melaj, M. A., & Daraio, M. E. (2013). Preparation and characterization of potassium nitrate controlled release fertilizer based on chitosan and xanthan layered tablets. *Journal of Applied Polymer Science*, *130*(4), 2422–2428.
Mi, F. L., Shyu, S. S., Lee, S. T., & Wong, T. B. (1999). Kinetic study of chitosan-tripolyphosphate complex reaction and acid-resistive properties of the chitosan-tripolyphosphate gel beads prepared by in-liquid curing method. *Journal of Polymer Science Part B: Polymer Physics*, *37*(14), 1551–1564.
Nge, K. L., Nwe, N., Chandrkrachang, S., & Stevens, W. F. (2006). Chitosan as a growth stimulator in orchid tissue culture. *Plant Science*, *170*(6), 1185–1190.
Ni, B., Lü, S., & Liu, M. (2012). Novel multinutrient fertilizer and its effect on slow release, water holding, and soil amending. *Industrial & Engineering Chemistry Research*, *51*(40), 12993–13000.
Pavlovic, S., & Brandao, P. R. G. (2003). Adsorption of starch, amylose, amylopectin and glucose monomer and their effect on the flotation of hematite and quartz. *Minerals Engineering*, *16*(11), 1117–1122.
Pawlak, A., & Mucha, M. (2003). Thermogravimetric and FTIR studies of chitosan blends. *Thermochimica Acta*, *396*(1), 153–166.
Pelissari, F. M., Grossmann, M. V., Yamashita, F., & Pineda, E. A. G. (2009). Antimicrobial, mechanical, and barrier properties of cassava starch-chitosan films incorporated with oregano essential oil. *Journal of Agricultural and Food Chemistry*, *57*(16), 7499–7504.
Pierog, M., Gierszewska-Drużyńska, M., & Ostrowska-Czubenko, J. (2009). Effect of ionic crosslinking agents on swelling behavior of chitosan hydrogel membranes. Progress on Chemistry and Application of Chitin and its Derivatives. *Polish Chitin Society, Łódź*, *75*, 82.
Qi, L., & Xu, Z. (2004). Lead sorption from aqueous solutions on chitosan nanoparticles. *Colloids and Surfaces A: Physicochemical and Engineering Aspects*, *251*(1), 183–190.
Qi, L., Xu, Z., Jiang, X., Hu, C., & Zou, X. (2004). Preparation and antibacterial activity of chitosan nanoparticles. *Carbohydrate Research*, *339*(16), 2693–2700.
Rashidzadeh, A., Olad, A., Salari, D., & Reyhanitabar, A. (2014). On the preparation and swelling properties of hydrogel nanocomposite based on Sodium alginate-g-poly(acrylic acid-co-acrylamide)/Clinoptilolite and its application as slow release fertilizer. *Journal of Polymer Research*, *21*(2), 1–15.
Rindlav-Westling, Å., Stading, M., & Gatenholm, P. (2002). Crystallinity and morphology in films of starch, amylose and amylopectin blends. *Biomacromolecules*, *3*(1), 84–91.
Liang, R., Liu, M., & Wu, L. (2007). Controlled release NPK compound fertilizer with the function of water retention. *Reactive & Functional Polymers*, *67*, 769–779.
Samanta, H., & Ray, S. (2014). Synthesis, characterization: swelling and drug release behavior of semi-interpenetrating network hydrogels of sodium alginate and polyacrylamide. *Carbohydrate Polymers*, *99*, 666–678.
Sarmento, B., Ferreira, D., Veiga, F., & Ribeiro, A. (2006). Characterization of insulin-loaded alginate nanoparticles produced by ionotropic pre-gelation through DSC and FTIR studies. *Carbohydrate Polymers*, *66*(1), 1–7.
Shaviv, A. (2001). Advances in controlled-release fertilizers. *Advances in Agronomy*, *71*, 1–49.
Shaviv, A., & Mikkelsen, R. (1993). Controlled-release fertilizers to increase efficiency of nutrient use and minimize environmental degradation—a review. *Fertilizer Research*, *35*(1–2), 1–12.
Shu, X. Z., & Zhu, K. J. (2001). Chitosan/gelatin microspheres prepared by modified emulsification and ionotropic gelation. *Journal of Microencapsulation*, *18*(2), 237–245.
Trenkel, M. (1997). . *Controlled-release and stabilized fertilizers in agricultura* (vol. 11) Paris: International Fertilizer Industry Association.
Tripathi, P., & Dubey, N. K. (2004). Exploitation of natural products as an alternative strategy to control postharvest fungal rotting of fruit and vegetables. *Postharvest Biology and Technology*, *32*(3), 235–245.
Valiela, I., Foreman, K., LaMontagne, M., Hersh, D., Costa, J., Peckol, P., et al. (1992). Couplings of watersheds and coastal waters: sources and consequences of nutrient enrichment in Waquoit Bay, Massachusetts. *Estuaries*, *15*(4), 443–457.
Wang, Q., Zhang, N., Hu, X., Yang, J., & Du, Y. (2007). Chitosan/starch fibers and their properties for drug controlled release. *European Journal of Pharmaceutics and Biopharmaceutics*, *66*(3), 398–404.
Xu, Y., Kim, K., Hanna, M., & Nag, D. (2005). Chitosan–starch composite film: preparation and characterization. *Industrial Crops and Products*, *21*(2), 185–192.
Yalinca, Z., Yilmaz, E., & Bullici, F. (2012). Evaluation of chitosan tripolyphosphate gel beads as bioadsorbents for iron in aqueous solution and in human blood in vitro. *Journal of Applied Polymer Science*, *125*(2), 1493–1505.
Zawadzki, J., & Kaczmarek, H. (2010). Thermal treatment of chitosan in various conditions. *Carbohydrate Polymers*, *80*(2), 394–400.
Zhiqiang, L., Xiao-su, Y., & Yi, F. (1999). Effect of bound water on thermal behaviors of native starch, amylose and amylopectin. *Starch-Stärke*, *51*(11–12), 406–410.
Zhong, K., Lin, Z., Zheng, X., Jiang, G., Fang, Y., Mao, X., et al. (2013). Starch derivative-based superabsorbent with integration of water-retaining and controlled-release fertilizers. *Carbohydrate Polymers*, *92*(2), 1367–1376.